# Numerical modeling of shear bands in rocks using FEM and a viscous regularization technique

Renan S. B. de Lima[1,2], Roberto Quevedo[1], Bruno R. B. M. Carvalho[3], Deane Roehl[1,2]

[1]*Tecgraf Institute, PUC-Rio*
*Rua Marquês de São Vicente, 225, 22453-900, Rio de Janeiro, Brazil*
*renanlima@tecgraf.puc-rio.br, rquevedo@tecgraf.puc-rio.br, deane@tecgraf.puc-rio.br*
[2]*Civil Engineering Department, PUC-Rio*
*Rua Marquês de São Vicente, 225, 22453-900, Rio de Janeiro, Brazil*
*renanlima@aluno.puc-rio.br, droehl@puc-rio.br*
[3]*Petrobras Research Center*
*Av. Horácio Macedo, 950, Cidade Universitária, Ilha do Fundão, 21941-915, Rio de Janeiro, Brazil,brcarvalho@petrobras.com.br*

**Abstract.** Shear bands are narrow zones of intense shear strain that develop within a broad range of ductile materials. As these bands precede material failure, their study is fundamental to understand the mechanical behavior of those materials. In general, the modelling of shear bands is performed through the finite element method considering constitutive laws which use a non-associative flow rule. Moreover, models for porous materials such as rocks and soils usually incorporate strain-softening behavior observed in experimental tests. Both non-associative flow rules and strain-softening can cause loss of well-posedness of the initial-value problem in classical continuum approaches, leading to mesh dependency and poor convergence during the non-linear solution process. To overcome such issues, some techniques such as viscous regularization have been proposed. However, the removal of mesh dependency depends on how the viscous parameter is incorporated into the model. In this paper, we present simulations of shear bands considering biaxial conditions and including a viscous regularization technique. The efficiency of that technique is studied considering the onset, width and orientation of the resultant shear bands in carbonate rocks. We show that despite the use of non-associative flow rules and strain-softening behavior, the obtained shear band widths converge to finite values upon increasing mesh discretization.

**Keywords:** Shear bands, Viscous regularization techniques, Finite element method.

## 1 Introduction

Shear bands is a ubiquitous phenomenon that occurs as consequence of intense shear strain in narrow bands preceding failure of several materials. That kind of localized deformation has been the focus of intense research since the middle of the 20$^{th}$ century, particularly in solid materials [1][2]. Shear bands in geomaterials has also received attention because of their consequences for reservoir engineering with impacts on the migration of fluids (water, oil or gas) in sedimentary basins [3][4]. For characterization of the mechanical behavior of porous materials, some laboratory tests are performed in plugs aiming the assessment of elastic and strength properties as well as the onset, width and orientation of shear bands. However, experimental tests have some disadvantages, such as insufficient sample quantity, time constraints, and associated costs. An alternative for characterization of shear bands is through numerical modeling using constitutive relationships based on plasticity theory. Moreover, for representative and more realistic behavior of the material, non-associative flow-rules and strain-softening are incorporated in the constitutive models. Unfortunately, with those features the material tangential operator locally loses positive-definiteness. This local instability can lead to the loss of ellipticity of the equilibrium equation becoming the problem ill-posed enabling instabilities and convergence problems. Therefore, methods based on

continuum mechanics such as the finite element method (FEM) fails to define the shear band domain where plastic deformations are confined, particularly when refined meshes are adopted, showing mesh dependent results [5]. In order to deal with those issues, some techniques have been proposed in the literature. This is the case of the viscous regularization technique that inserts an implicit intrinsic parameter with length scale in the constitutive relations that define the size of the region with localized deformations. Viscous regularization consists of introducing time-dependent behavior into the material and allows the regularization of any elastoplastic material [6]. It is based on the fact that localization causes high deformation rates, which are reduced and distributed in the finite element mesh by means of the viscosity [7]. However, the capabilities and impacts of using the viscous regularization technique on the development of shear bands in geomaterials have not been discussed. Therefore, in this study, we present a numerical methodology based on FEM, plasticity theory and the viscous regularization technique for the characterization of shear bands in carbonate rocks. Through several simulations considering biaxial conditions, we show that viscous regularization is able to reduce mesh dependency. Moreover, we perform a sensitivity study for the assessment of the viscosity parameter.

## 2 Model description

The model used to represent the initiation of shear bands in a plug scale is shown in Fig. 1. It was generated in the commercial finite element package Abaqus® considering large displacements and plane strain conditions. Following the steps performed in laboratory tests, the sample is initially subjected to hydrostatic pressure ($\sigma_c$ =10 MPa), followed by incremental vertical displacements (U2) at model top, up to a maximum value of 4.0 mm. The displacements of the nodes at the bottom of the sample are restricted in both horizontal and vertical directions, while displacements at the nodes at the top are restricted horizontally. The mechanical behavior of the rock is represented by the Concrete Damaged Plasticity (CDP) constitutive model, which had its yield function manipulated to match the classical Drucker-Prager failure criterion (linear failure surface in the meridional plane and circular in the deviator plane). The reader is referred to Lima [8] for more information on this procedure and its verification. The CDP model was chosen because its implementation in ABAQUS includes a viscous regularization technique based on a generalization of the Duvaut-Lions regularization. The regularization is activated by setting a viscosity parameter named *relaxation time*.

Strain softening is considered by reducing the friction angle, the dilation angle and the cohesion according to the evolution of plastic deviatoric strains (eq. (1)). The reduction of those parameters occurs exponentially, as shown in Fig. 2. The initial value of the dilation angle was defined as 20º less than the friction angle [9]. The residual value was defined as 1.0º to limit the volumetric plastic strains at high strains [10]. The properties adopted in the models are shown in Tab. 1 and were obtained through laboratory tests carried out in the LEM-DEC Laboratory (PUC-Rio) considering Indiana Limestone samples. The residual properties were defined by Lima [8] and are also shown in Tab. 1. The finite element mesh is composed of eight-node quadrilateral elements with nine-point Gauss integration.

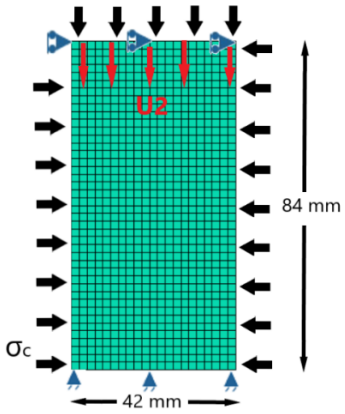


Figure 1. Geometry, mesh, and boundary conditions of finite element models.

$$E_d^p = \sqrt{\frac{3\left(\left(\varepsilon_{xx}^p\right)^2+\left(\varepsilon_{yy}^p\right)^2+\left(\varepsilon_{zz}^p\right)^2\right)}{2}+\frac{3\left(\left(\gamma_{xy}^p\right)^2+\left(\gamma_{yz}^p\right)^2+\left(\gamma_{zx}^p\right)^2\right)}{4}} \tag{1}$$

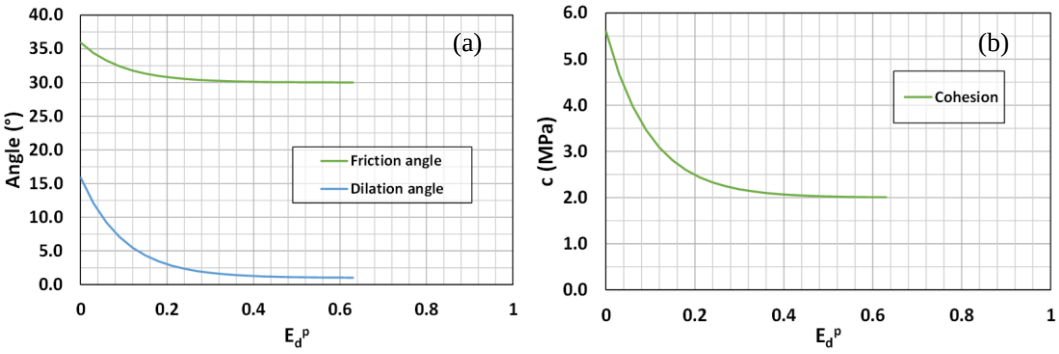


Figure 2. Reduction of selected parameters: (a) friction and dilation angles; (b) cohesion.

Table 1. Properties of the Indiana Limestone rock

| | Nomenclature | Initial value | Residual value |
|---|---|---|---|
| Young's modulus (GPa) | E | 23.46 | 23.46 |
| Poisson's ratio (-) | ν | 0.24 | 0.24 |
| Cohesion (MPa) | c | 5.60 | 2.00 |
| Friction angle (°) | φ | 35.91 | 30.00 |
| Dilation angle (°) | ψ | 15.91 | 1.00 |

In order to identify the initiation of shear bands, we choose the scalar variable PEMAG that represents the magnitude of plastic strain given in eq. (2).

$$PEMAG = \sqrt{2/3(PE_{P1}{}^2 + PE_{P2}{}^2 + PE_{P3}{}^2)} \tag{2}$$

where $PE_{P1}$, $PE_{P2}$ and $PE_{P3}$ are the principal accumulative plastic strains. We assume that the shear band domain is characterized by the occurrence of plastic deformations and defined by a region in which the value of PEMAG is greater than or equal to 0.1. Figure 3 describes the procedure for measuring the shear band width. Along a vertical path created at the bottom right of the models, we measure the evolution of PEMAG and then we define its width, considering the orientation of the shear band.

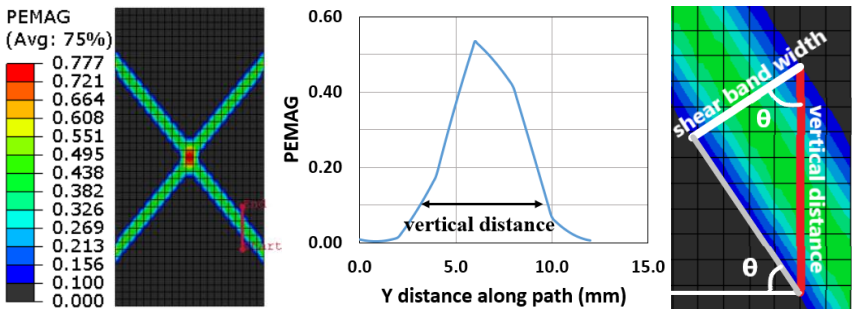


Figure 3. Measurement of the shear band width through PEMAG.

# 3 Mesh sensitivity study

A sensitivity study was carried out in order to investigate mesh dependency and analysis convergence in strain localization simulations. For this purpose, numerical simulations were performed with and without viscous regularization. The tested meshes have element sizes equal to 1.0 mm, 1.5 mm, 2.0 mm, 3.0 mm, 4.0 mm. In analyzes that rely on viscous regularization, the influence of relaxation time on model response was also studied. In these analyses, the relaxation time varied between the values 0.01 s, 0.02 s and 0.03 s. Lastly, an ideal relaxation time (μ) is determined.

## 3.1 Mechanical response, shear band width, shear band inclination and convergence

Table 2 exhibits the shear band inclination of simulations with and without viscous regularization. The model without regularization presents a reduction in this angle with the increase of the element size, and the difference between the largest and smallest angle is 3.0°. Therefore, shear band slope is also mesh dependent. The regularized models do not show this dependence of inclination in relation to mesh refinement. The maximum difference from the largest to the smallest inclination angle in the regularized models is 2.0°. It is considered that viscous regularization is also able to reduce mesh dependency on shear band slope.

Table 2. Properties of the carbonate rock

| μ | θ(°) as function of element size | | | |
|---|---|---|---|---|
| | 1.5 mm | 2.0 mm | 3.0 mm | 4.0 mm |
| 0.00 | 52.0 | 51.0 | 49.0 | 49.0 |
| 0.01 | 49.5 | 51.0 | 50.0 | 49.0 |
| 0.02 | 49.0 | 50.5 | 50.5 | 50.0 |
| 0.03 | 50.0 | 50.0 | 50.5 | 49.5 |

Figure 4 exhibits deviatoric stress-axial strain ($\sigma_d$-$\varepsilon_a$) curves. In the case without regularization, Fig. 4 (a), it is evident that after peak different discretization give different load capacities. The more refined the mesh, the more intense is the reduction of deviatoric stress in relation to axial strain and smaller is the residual deviatoric stress. This behavior indicates that model response is mesh dependent. When using viscous regularization (Fig. 4 (a, b, c)), an approximation of the $\sigma_d$-$\varepsilon_a$ curves and of the residual stresses for different discretization can be noticed as the relaxation time is increased. It is then considered that viscous regularization is able to reduce mesh dependency. Regularization also generates an increase in peak stresses, peak axial strains and residual stresses.

Observing the graphs in Fig. 5, which display shear band width in relation to the imposed vertical displacement, it can be seen that simulations without regularization (Fig. 5 (a)) present distinct shear band initiation and evolution. This behavior highlights the model's mesh dependency. When using viscous regularization (Fig. 5 (a, b, c)), it is noted that there is an approximation of the initial vertical displacements and of the initial shear band widths, as well as of the final shear band widths. For the case μ=0.02 s, the shear band width of 1.5 mm and 2.0 mm discretization become very close to each other. When a relaxation time greater than 0.02 s is used (Fig. 5 (d)) the simulation with the finest mesh has a final shear band width greater than simulations with less refined mesh. In the simulations with viscous regularization, the finest mesh (1.0 mm element) presented a double "X" shaped shear band configuration, different from the expected configuration as shown in Fig. 3. This behavior indicates that mesh refinement influences viscous regularization efficiency. Despite this limitation, it is considered from the analysis of the LB-D graphs that viscous regularization was able to reduce mesh dependency.

In all analyses, the total prescribed displacement (4.0 mm) was applied in 200 increments. Each increment can be subdivided according to analysis requirements. For this, a minimum sub-increment of $10^{-6}$ mm was defined. All simulations using viscous regularization were completed in 200 increments. On the other hand, the simulations without regularization and 1.0 mm and 1.5 mm discretization needed, respectively, 327 and 204 increments to be completed. From these data, it is concluded that viscous regularization improves convergence of the analysis.

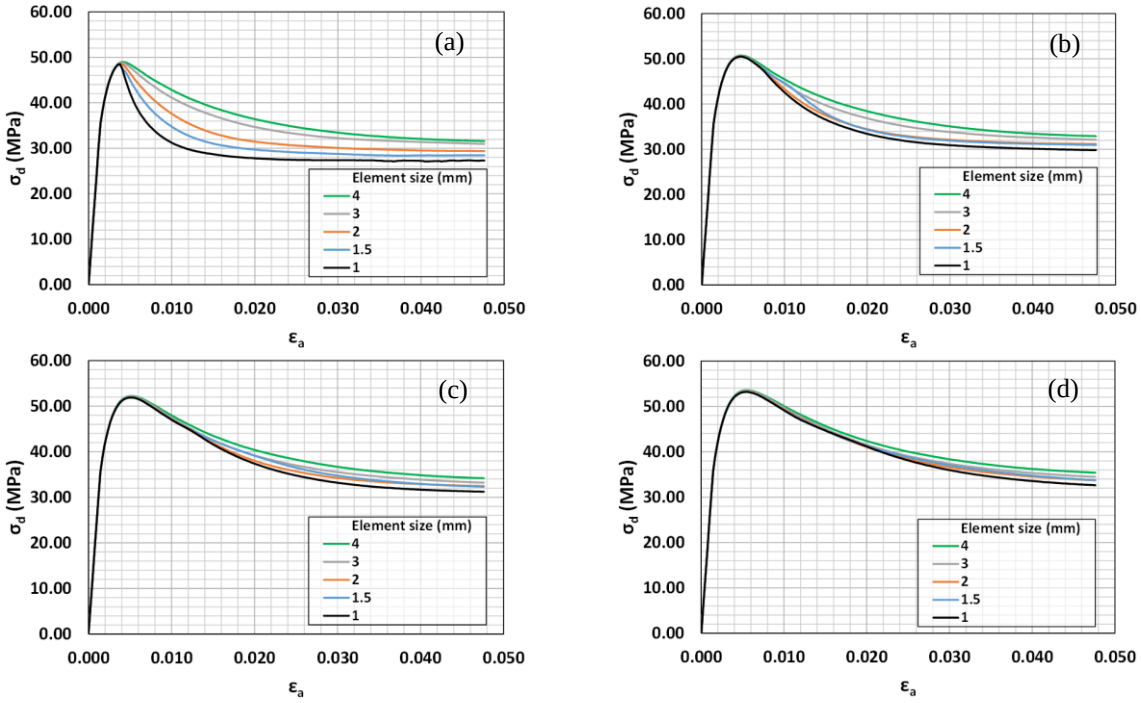


Figure 4. Deviatoric stress-axial strain curves ($\sigma_d$-$\varepsilon_a$) varying relaxation time: (a) μ=0 s; (b) μ=0.01 s; (c) μ=0.02 s; (d) μ=0.03 s.

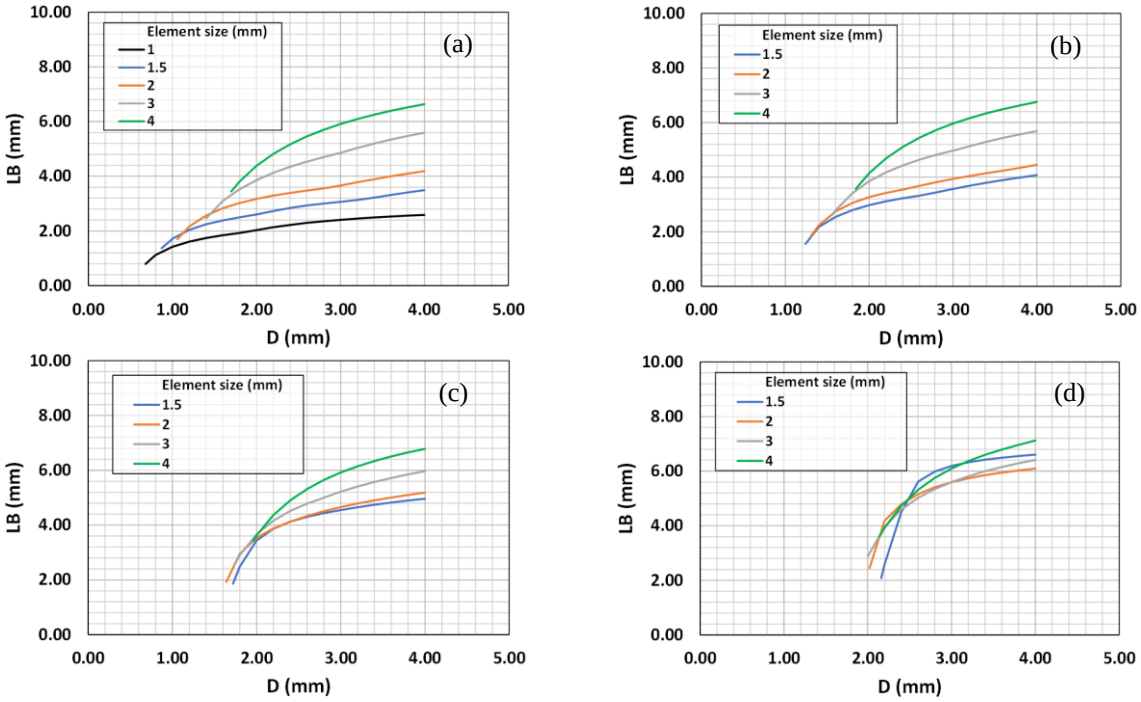


Figure 5. Shear band width-vertical displacement curves (LB-D) varying the relaxation time: (a) μ=0 s; (b) μ=0.01 s; (c) μ=0.02 s; (d) μ=0.03 s.

### 3.2 Ideal relaxation time

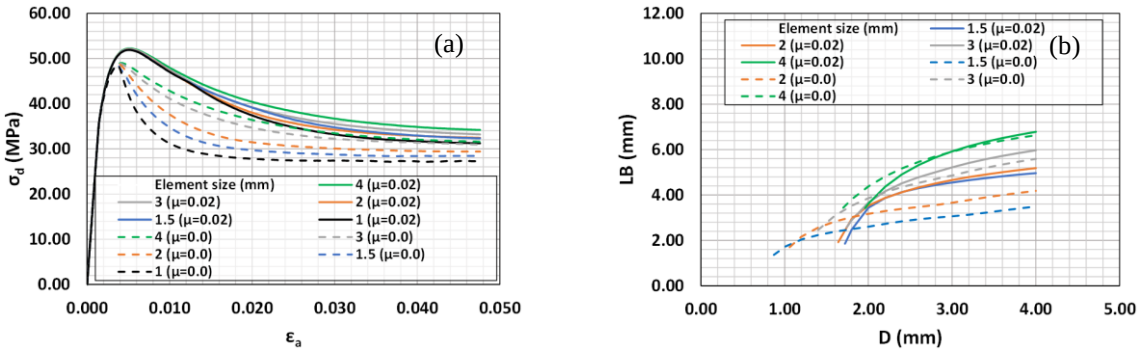


Figure 6. Comparison between different discretization with μ=0 s e μ=0.02 s for curves of: (a) deviatoric stress-axial strain ($\sigma_d$-$\varepsilon_a$); (b) shear band width-vertical displacement (LB-D).

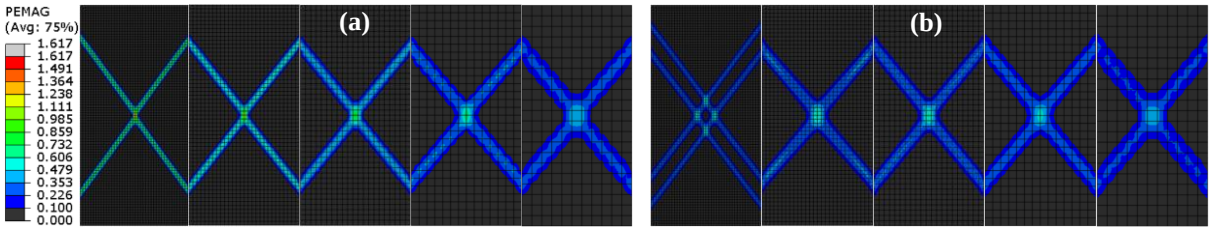


Figure 7. Comparison between PEMAG visualization of different discretization (from the finest on the left to the coarsest on the right in each set): (a) μ=0 s; (b) μ=0.02 s.

To define the ideal relaxation time, the influence of this parameter on the mechanical response of the material and on the evolution of the shear band width was taken into account. The ideal value of the relaxation time should not be so large as to raise the peak stress excessively, but it should be large enough to approximate stress-strain curves of different discretization. When the relaxation time is greater than 0.02 s, shear band widths do not converge; the finer discretization (1.5 mm element) presents a final shear band width greater than the less refined discretization (2.0 mm and 3.0 mm). Relaxation time less than 0.02 does not provide a satisfactory approximation of shear band width evolution curves. For these reasons and due to the convergence of shear band widths evolution of the 1.5 mm and 2.0 mm meshes, the ideal relaxation time was selected as 0.02 s. The effect of using viscous regularization compared to conventional continuum in mechanical response can be seen through Fig. 6 (a), while the same effect can be seen in shear band width evolution from Fig. 6 (b). The PEMAG contour plot (Fig. 7) visually presents what was graphically represented in Fig. 6 (b). It can be seen in Fig. 7 (b) that for the 1 mm element size mesh, the model presents the double “X” shear band pattern mentioned before. On the other hand, it is evident that the use of viscous regularization approximates the curves of different mesh discretization, both in terms of mechanical response and shear band width evolution.

## 4 Conclusions

This work proposes a methodology for shear band characterization in geomaterials using FEM, plasticity theory and a viscous regularization technique. From the numerical results, it was demonstrated that the viscous regularization is effective and manages to reduce mesh dependency in shear band width, mechanical response, and shear band slope. However, a limitation of this technique was noted when using extremely fine meshes. In these situations, shear bands presented a double "X" pattern. This indicates that viscous regularization does not eliminate response sensitivity to the mesh. A lower bound to element size should be established to enhance its effectiveness. Although viscous regularization improved the performance of the model, it was not able to totally eliminate mesh sensitivity. In addition, it requires extensive testing to define the adequate relaxation time and mesh size. For this reason, a study was carried out to define the ideal value for this parameter, which for the proposed model is 0.02s.

**Acknowledgements.** This research was carried out in association with the ongoing R&D project registered as ANP n° 21475-9, "GeoBanD – Geomodelagem de zona de dano em falhas geológicas" (PUC-Rio/CENPES/ANP), sponsored by Petrobras. The authors also gratefully acknowledge the support from Coordenação de Aperfeiçoamento de Pessoal de Nível Superior (CAPES).

**Authorship statement.** The authors hereby confirm that they are the sole liable persons responsible for the authorship of this work, and that all material that has been herein included as part of the present paper is either the property (and authorship) of the authors, or has the permission of the owners to be included here.

## References

[1] Yadav, S. and Sagapuram, D. (2020) 'In situ analysis of shear bands and boundary layer formation in metals', Proceedings of the Royal Society A: Mathematical, Physical and Engineering Sciences, 476(2234). doi: 10.1098/rspa.2019.0519.
[2] Zhang, H. et al. (2021) 'Phase-field modeling of spontaneous shear bands in collapsing thick-walled cylinders', Engineering Fracture Mechanics. Elsevier Ltd, 249(March), p. 107706. doi: 10.1016/j.engfracmech.2021.107706.
[3] De Araújo Netto, J. M., Da Silva, F. C. A. and De Sá, E. F. J. (2012) 'Caracterização meso e microscópica de bandas de deformação em arenitos porosos: um exemplo nas tectonossequê ncias Paleozoica, Pré- e Sin-rifte da Bacia do Araripe, Nordeste do Brasil', Geologia USP - Serie Cientifica, 12(1), pp. 83–98. doi: 10.5327/Z1519-874X2012000100007.
[4] Fossen, H. et al. (2007) 'Deformation bands in sandstone: A review', Journal of the Geological Society, 164(4), pp. 755–769. doi: 10.1144/0016-76492006-036.
[5] Sharbati, E. and Naghdabadi, R. (2006) 'Computational aspects of the Cosserat finite element analysis of localization phenomena', Computational Materials Science, 38(2), pp. 303–315. doi: 10.1016/j.commatsci.2006.03.003.
[6] Cardoso, R. S. and Varum, H. (2006) 'Visco-elastic regularization and strain softening', III European Conference on Computational Mechanics, (August 2015). doi: 10.1007/1-4020-5370-3.
[7] da Silva, V. D. (2004) 'A simple model for viscous regularization of elasto-plastic constitutive laws with softening', Communications in Numerical Methods in Engineering, 20(7), pp. 547–568. doi: 10.1002/cnm.700.
[8] Lima, R. S. B. De (2021) Modelagem Computacional de Bandas de Deformação em Escala de Plugue. Pontifícia Universidade Católica do Rio de Janeiro.
[9] Vermeer, P. A. and De Brost, R. (1984) 'Non-associated plasticity for soils, concrete and rock', Heron, 29.
[10] Alejano, L. R. et al. (2009) 'Ground reaction curves for tunnels excavated in different quality rock masses showing several types of post-failure behaviour', Tunnelling and Underground Space Technology. Elsevier Ltd, 24(6), pp. 689–705. doi: 10.1016/j.tust.2009.07.004.